Arabian Journal of Chemistry (2022) **15**, 103650

King Saud University

Arabian Journal of Chemistry

www.ksu.edu.sa
www.sciencedirect.com

ORIGINAL ARTICLE

Insight into the extraction and characterization of cellulose nanocrystals from date pits

Sara A. Wahib, Dana A. Da'na, Mohammad A. Al-Ghouti *

Environmental Science Program, Department of Biological and Environmental Sciences, College of Arts and Sciences, Qatar University, State of Qatar – Doha. P.O. Box: 2713, Qatar

Received 18 September 2021; accepted 13 December 2021
Available online 17 December 2021

KEYWORDS

Agricultural wastes;
Cellulose nanocrystals;
Bio-based nanoscale products

Abstract This study aims to extract and characterize cellulose nanocrystals (CNCs) from date pits (DP), an agricultural solid waste. Two methods were used and optimized for the cellulose nanocrystals (CNCs) extraction, namely the mechanical stirrer method ($CNCs_1$) and the Soxhlet apparatus method ($CNCs_2$) in terms of chemical used, cost, and energy consumption. The results showed that scanning electron microscopy revealed the difference in the morphology as they exhibit rough surfaces with irregular morphologies due to the strong chemical treatments during the delignification and bleaching process. Moreover, transmission electron microscopy analysis for CNCs reveals the true modification that was made through sulfuric acid hydrolysis as it presents cellulose microfibrils with a packed structure. Fourier transform infrared proved that the CNCs were successfully extracted using the two methods since most of the lignin and hemicellulose components were removed. The crystallinity index of $CNCs_1$ and $CNCs_2$ was 69.99%, and 67.79%, respectively, and both presented a high yield of CNCs ($\geq$10%). Ultimately, both techniques were successful at extracting CNCs. Based on their cost-effectiveness and time consumption, it was concluded that method 1 was less expensive than method 2 based on the breakdown of the cost of each step for CNCs production.

1. Introduction

Over the years, the usage of crystalline cellulose in material production has spiked an interest in research fields. Such organic biopolymers can be used as a strengthening material with other polymers because of their unique characteristics like their high thermal and mechanical stability, biodegradability nature, and low toxicity towards the environment (Dharmalingam et al., 2019; Medina et al., 2019; Ferreira et al., 2018; Khalil et al., 2018). Different kinds of cellulose particles can be extracted from cellulose materials, such as cellulose nanocrystals (Khan et al., 2020; Kian et al., 2019; Wang et al., 2019; Zheng et al., 2019) or sometimes called cellulose nanowhiskers (Araki & Miyayama, 2020; Jafari et al., 2020; Khattab et al., 2020). Others also include microcrystalline cellulose (Abu-Thabit et al. 2020; Alavi, 2019) and microfibril-

* Corresponding author.
E-mail address: mohammad.alghouti@qu.edu.qa (M.A. Al-Ghouti).
Peer review under responsibility of King Saud University.

Production and hosting by Elsevier

https://doi.org/10.1016/j.arabjc.2021.103650
1878-5352

lated cellulose (Silva et al., 2020; Li et al., 2018). The source of cellulose material and the extraction methods are important factors that determine the crystallinity, crystal structure, aspect ratio, and morphology of the extracted cellulose particles (Trache et al., 2016; Deepa et al., 2015). Previous researches have shown the possibility of cellulose and nanocellulose extraction from various sources, such as wood paste (Dong, 2016), pistachio hull (Marett et al., 2017), pine and corn bark (Ditzel et al., 2017), wood (Rajinipriya et al., 2018), ramie (Syafri et al., 2018), bagasse (Li et al., 2012), bamboo (Brito et al., 2012), Rice husk (Fathi et al., 2018), mulberry (*Morus alba* L.) (Li et al., 2009), sisal and cotton fibers (Magalhães et al., 2009) and many others. Moreover, locally available solid wastes, such as date pits, are an excellent source for extracting cellulose since they contain as much as 42% cellulose (Ogungbenro et al., 2018).

Investigators have been trying to come up with a way to use raw materials, which are economically and environmentally friendly. Therefore, the usage of cellulose, as a biopolymer and a sustainable raw material, is the most appropriate choice because of its abundance found on earth (Abu-Thabit et al., 2020; Etale et al., 2020). Furthermore, Wahib et al. (2021) successfully prepared a novel adsorbent that contains cellulose nanocrystals (CNCs) extracted from date pits (DP) and ionic liquid (IL) and then loaded it onto a date pit to prepare IL-CNC@DP adsorbent. This study also investigated the ability of this adsorbent to remediate boron in comparison to the unmodified date pits. The data indicated the superiority of IL-CNC@DP over DP in which their maximum adsorption capacities were 97 and 69 mg/g, respectively. This was due to the greater surface area of IL-CNC@DP which was 4.254 m/g compared to 2.126 m/g for DP. Moreover, the results revealed that the removal efficiency of boron from water peaked and reached 97% at pH 6, and there was no change detected with the change of solution temperature for both adsorbents. Moreover, Another study has been conducted by Hosseini et al. (2020) to investigate the adsorption mechanism of Pb (II), Hg (II), and Cr (VI) ions onto ultra-lightweight, porous, durable, 3D-cryogel based adsorbent by integrating 10% GO and Fe_3O_4 nanoparticles into CNFs (cellulose nanofibrils) extracted from date palm waste as a major source of cellulose. Hosseini et al. (2020) used freeze-drying, which is an eco-friendly and affordable method, to successfully prepare CNFs/GO/ Fe_3O_4 bionanocomposite cryogels. The results of the study confirmed the great uptake performance of the novel adsorbent of Pb (II), Hg (II), and Cr (VI), and their adsorption capacities are 126.58 mg/g, 36.70 mg/g, and 73.52 mg/g, respectively. The authors also confirmed that CNFs/GO/ Fe_3O_4 bionanocomposite cryogel adsorbent can be considered as a suitable candidate to treat effluents that are contaminated with heavy metal ions due to its ultra-porosity structure, suitable thermal and mechanical properties, low density, green synthetic way, and supreme adsorption.

The process of obtaining cellulose on the nanoscale can be performed mechanically or chemically by modifying the type of polymer used (Börjesson & Westman, 2015). This nanofiber possesses a biodegradable property with low density and an impressive firmness material (Phanthong et al., 2018). Comparing cellulose to nanocellulose, nanocellulose polymers have high crystallinity, high mechanical strength, and high hydrophilicity (Zheng et al., 2019). Moreover, those cellulose nanomaterials with high surface-to-volume ratio, biodegradability, high functionalizability, and sustainability hold great potential in water treatment after already demonstrating their application in paper and packaging, textile industries, and other fields (Carpenter et al., 2015). Nanocellulose is employed in a variety of applications. For example, enhancement of mechanical and barrier properties of interior panels in automotive is one of the applications of nanocellulose (Lyne, 2013). Other types of applications include the use of nanocellulose in cement or concrete construction (Ardanuy Raso et al., 2012). As for small-scale applications, nanocellulose can be used in aerogel production, as they are efficient in absorbing oil from water (Cervin et al., 2012). Furthermore, industrial activities make use of nano-products since they are used as viscosity modifiers that can reduce oil thinning as temperature increases. They are used in water purification by the adsorption process (Dufresne, 2017). Regardless, it is safe to say that one of the most promising approaches for nanocellulose applications is its employment as a filler in biocomposites. The integration of these bio-composites and their excellent characteristics, as previously mentioned, along with their relatively low production cost can be a promising method towards the next generation of green materials. This is due to the properties in which they possess rod-shaped morphologies with a large surface area that ranges from 150 m^2/g – 250 m^2/g with low density at 1.566 g/cm^3 and a high aspect ratio of 10 – 85 (Shafizah et al., 2018). Furthermore, they possess nano sectional fibers with nano dimensional cross-sectional morphologies making them excellent candidates for various applications (Isogai et al., 2011).

There are several sources mentioned where cellulose can be obtained from either crop, industrial residues, or animal residues. The biomass extracted has three main components, namely cellulose, hemicellulose, and lignin (Díez et al., 2020; Jung et al., 2015; Isik et al., 2014). Each cellulose fibril is made up of a crystalline and amorphous (non-crystalline) region (Song et al., 2014). To obtain the crystalline region to produce cellulose nanocrystals (CNCs), the amorphous region of cellulose fibers needs to be separated (Brinchi et al., 2013). Therefore, extraction of CNCs normally consists of two processes, chemical purification, and acid hydrolysis. The cellulose source and extraction process determine the properties of the cellulose polymer; likewise, nanocellulose depends upon the same factors (Deepa et al., 2015; Sacui et al., 2014). Therefore, such factors can help determine the different classifications of nanocellulose. In general, nanocellulose can be classified into three types of materials, namely nanocrystalline cellulose (NCC) or cellulose nanocrystals (CNCs), nanofibrillated cellulose (NFC), and bacterial nanocellulose ones (BNC) (Kian et al., 2019; Kontturi et al., 2018; Jawaid et al., 2017; García et al., 2016). Even though such materials are the same regarding their chemical structure, they differ in their morphologies and treatment methods. According to numerous researchers, there are various methods for the production of CNCs such as mechanical method, ionic liquid method, enzymatic method, 2,2,6,6-Tetramethylpiperidine-1-oxyl radical (TEMPO) oxidative method, combination method (oxidative or enzymatic and mechanical), acid hydrolysis by different acids, such as sulfuric acid, phosphoric acid, and hydrochloric acid (Guo et al., 2020; Ribeiro et al., 2020; Ribeiro et al., 2019; Peretz et al., 2019). Table 1 discusses three main CNCs extraction methods.

Table 1 Methods used for CNCs extraction.

Method	Advantages/disadvantages	Yield (%)	Reference
Acid hydrolysis	CNCs with excellent suspension stability. Difficult to treat acid waste.	15.7	Cheng et al., 2017
Enzymatic hydrolysis	Environmentally friendly. High cost.	13.6	Meyabadi et al., 2014
Oxidation degradation	High consumption of oxidants. Production of CNCs carboxylation.	35	Yang et a., 2013
Mechanical process	High crystallinity and thermal stability.	85.35	Tang et al., 2013

Among all these methods, acid hydrolysis by sulfuric acid has been known as the most widely used method for CNCs extraction due to its simplicity as well as resulting in the nanoparticle of 100–1000 nm with high crystallinity and stiffness (Wulandari et al., 2016; Börjesson & Westman, 2015; Shanmugarajah et al., 2015; Lani et al., 2014). Moreover, the Soxhlet extraction method has multiple advantages, for example, the sample phase is repeatedly brought into contact with a fresh portion of the solvent, thereby enhancing the displacement of the analyte from the matrix as well as no filtration is required after the leaching step, requires inexpensive equipment, very simple methodology and has the possibility to extract more sample mass compared to the latest extraction methods. However, this method also has major drawbacks such as the long time required for the extraction as well as the large amount of organic solvent wasted which is expensive to dispose of and can cause environmental pollution (Luque-Carcia and De Castro, 2004). The mechanical stirrer is the most popular among all extraction techniques proposed in recent years for reducing wastes (Camino-Sanchez et al., 2014). Therefore, this study aims to extract and characterize the CNCs from date pits (DP) using the sulfuric acid hydrolysis through the Soxhlet apparatus technique and mechanical stirrer technique accompanied with ultrasonication. Furthermore, comparing the produced CNCs by both methods as well as their costs. The chemical components, morphology, crystallinity, and physicochemical properties of the prepared CNCs were also investigated. Moreover, since environmental conservation is a growing concern, it encouraged researchers to develop biodegradable materials from natural sources for various applications. Different studies focused on utilizing agricultural wastes to obtain more valuable materials, which can be applied in sustainable applications. The uniqueness of this paper presents how using residual biomass benefits the use of waste products as well as provides new renewable materials. Hence, in this study, date pits are used due to their plentiful local availability found as agricultural waste in Qatar. Therefore, it is used to simultaneously reduce the amount of date pits wastes and to isolate the CNCs. Based on our knowledge, no previous studies have reported the extraction and characterization of cellulosic materials from date pits (DP) except for our previous publications (Wahib et al., 2021; Wahib et al., 2022).

2. Methodology

2.1. Materials

Qatari date fruits, *Phoenix dactylifera* L. were collected from local stores in Qatar. Sodium hydroxide (research lab fine chem industries, India), sodium hypochlorite (Alfa Aesar, the United States), n-hexane (Scharlab S.L., Spain), and sulfuric acid (Sigma-Aldrich, United States) were of analytical grade and used without any further purification. Distilled water was used in the whole process. Dialysis bags were provided by Carolina Biological Supply Company.

2.2. Preparation of starting material

The date pits (DP) samples were washed with distilled water to remove any dirt and impurities. The samples were left overnight to air dry. A microphyte disintegrator was utilized for the grinding of DP. After that, the samples were stored at room temperature for future use.

2.3. Extraction of cellulose and cellulose nanocrystals from date pits

The schematic illustration of the used extraction methods for cellulose nanocrystals (CNCs) from the DP is shown in Fig. 1.

2.3.1. Method 1-Mechanical stirrer

Five hundred milliliters of 6.0 % sodium hydroxide (NaOH) were prepared in an Erlenmeyer flask with 50 g of ground DP to delignify the samples. This mixture was heated at 70 °C and stirred for 4 hrs using the mechanical stirrer. A neutral pH value has been achieved after filtering the black lignin waste with a constant washing of the solid part by using distilled water. The mixture was left to air dry overnight and the product attained after the NaOH treatment is denoted as N_1-DP. Furthermore, the neutralized mixture undergoes bleaching by the addition of 300 mL of 6.0% sodium hypochlorite solution (NaClO). The mixture was stirred for 2 hrs at 70 °C using the mechanical stirrer and the solid part was filtered off from the liquid. Then, the product has undergone further bleaching around six times, consecutively, before washing the product exhaustively with distilled water to afford neutral cellulose. After that, it was separated by filtration, and the obtained solid product was cellulose (Lusiana et al., 2019). Finally, the pure cellulose was left to air dry overnight for further use and the product attained after the NaClO treatment is denoted as B_1-DP.

2.3.2. Method 2-Soxhlet apparatus

In this method, 50 g of ground DP were dewaxed in a Soxhlet apparatus using 500 mL of 96% n-hexane in several cycles for 8 hrs. The black concentered hexane extract of this step was left to evaporate under reduced pressure. Then, it was followed by further washing by 500 mL of distilled water for 8 hrs in

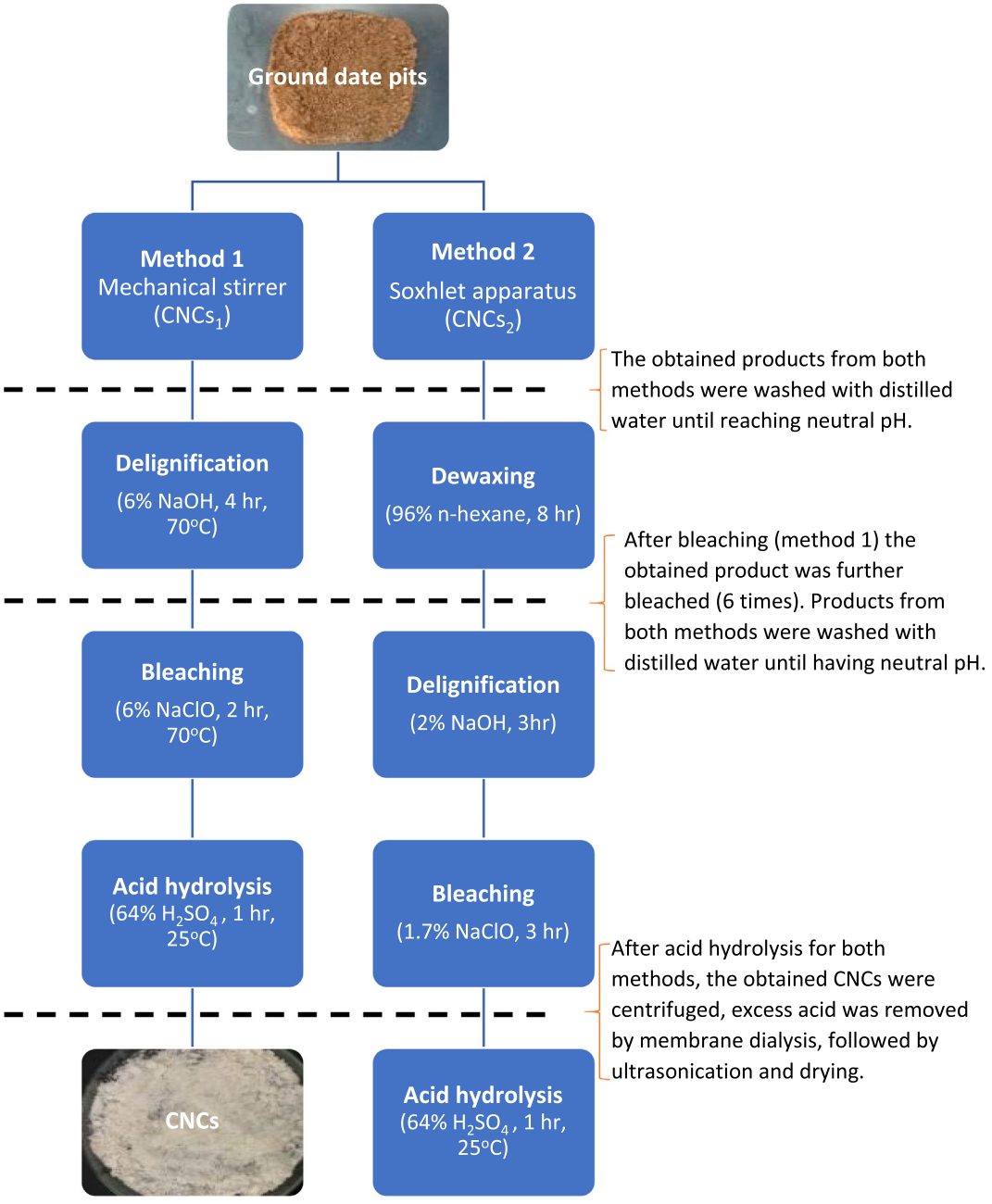

Fig. 1 Extraction methods of CNCs from the DP.

several cycles in the Soxhlet extractor. Afterward, the dewaxed fibers of the DP were left to air-dry overnight. To delignify the DP, 500 mL of 2.0% sodium hydroxide (NaOH) were added in the Soxhlet extractor with the dewaxed DP for the alkaline extraction step for 3 hrs. The product was then consecutively washed with distilled water to afford neutral delignified cellulose and was left to air dry overnight and the product is denoted as N_2-DP. The final step is bleaching by 1.7% of NaClO in the Soxhlet extractor for 3 hrs (Nabili et al., 2016). The solid product was washed with distilled water to afford neutral cellulose and was left to air dry overnight and the product is denoted as B_2-DP.

2.4. Preparation of cellulose nanocrystals (CNCs)

According to our preliminary research, the obtained cellulose from methods 1 and 2 was subjected to 500 mL of 64% sulfuric acid (H_2SO_4) for 1 hr under 25 °C (Wahib et al., 2022). The reaction ended by adding cold distilled water that is 10 times the volume of the reaction. Then, neutral pH was achieved by repetitive washing of sulfuric acid with distilled water. After that, separation of CNCs has been carried out by using the centrifuge for 30 mins at 5000 rpm. Moreover, the excess sulfate ions were removed by using a dialysis membrane in which the CNCs were soaked in distilled water for 48 hrs, which then

has been followed by ultrasonication for another 15 mins at 600 w. Finally, an oven was used to dry the obtained CNCs at 70 °C overnight. The CNCs obtained by method 1 will be denoted as $CNCs_1$ and by method 2 as $CNCs_2$.

2.5. Characterization of CNCs and intermediate products

2.5.1. Chemical composition measurement of the lignocellulosic materials of the DP

The chemically-treated DP was measured in accordance with the standards of the Technical Association of Pulp and Paper Industry (TAPPI) for the chemical composition of each intermediate product of each method (N_1-DP, B_1-DP, N_2-DP, and B_2-DP). Two samples from each method were tested and the average values were obtained in the end. The holocellulose content, which comprises cellulose and hemicellulose, was determined according to the method described in TAPPI T19m-54. To determine the α-cellulose content, treatment by NaOH of the fiber was done to remove the hemicellulose. Furthermore, the difference between the holocellulose and α-cellulose values gives the hemicellulose content. Lastly, the lignin content was also analyzed by using sulfuric acid in accordance with the standard method TAPPI-T222 cm-99. The obtained values are then compared with the original content of DP as mentioned by Al-Ghouti et al., (2019).

2.5.2. Determination of physical properties of the extracted CNCs from methods 1 and 2

True density, moisture content, and pH were determined for CNCs from both methodologies. The true density was determined by using the liquid displacement method that has been previously described by Abu-Thabit et al. (2020). Immersion liquid xylene was used, and the true density (D_T) was calculated by the Eq. (1):

$$D_T = \frac{w}{[(a+w)-b]} \times SG \tag{1}$$

Where w is the mass of the CNCs sample, SG is the specific gravity of xylene, a is the total mass of the (pycnometer bottle + solution), and b is the sum of the mass of the (pycnometer bottle + solution + sample). The results were based on two duplicates and their average was reported. The experiment was done for both methodologies. Furthermore, moisture content was carried out following the procedure of Tarchoun et al., (2019). The moisture content (MC) was calculated using Eq. (2).

$$MC(\%) = [\frac{wi - wf}{wi}] \times 100 \tag{2}$$

Where w_i is before drying the sample (g) and w_f is after drying the sample (g). The results were based on two duplicates and their average was reported. The experiment was done for both methodologies. Also, the pH was determined relying on the method by Kambli et al., (2017). The CNCs sample was immersed in 500 mL of distilled water. Then the suspension was placed on the shaker for 30 min at 25 °C. A portable digital pH meter was used to determine the suspension pH for both methodologies.

Lastly, the yield of $CNCs_1$ and $CNCs_2$ were calculated according to the gravimetric analysis method as demonstrated by Seta et al. (2020).

The equation of yield of both CNCs samples is calculated as per Eq. (3).

$$Yield(\%) = [\frac{W2}{W1}] \times 100 \tag{3}$$

Where W_2 is the weight of the final dried samples and W_1 is the dry weight of the initially dried DP. The results were based on two duplicates and their average is reported.

2.5.3. Characterization of the prepared materials

To understand the involved processes and mechanisms, it is important to characterize the prepared materials. Therefore, the characteristics of the materials (DP, N_1-DP, B_1-DP, N_2-DP, B_2-DP, $CNCs_1$, and $CNCs_2$) were determined. The morphological characteristics of the material's surface were evaluated by scanning electron microscope (SEM) (JEOL model JSM-6390LV). The obtained CNCs from both methods after drying was then mounted on a conductive carbon tape before coating the sample with gold to analyze by SEM. Furthermore, Fourier transform infrared (FTIR) spectra of $CNCs_1$ & $CNCs_2$ were recorded using the RSpirit-T model. The FTIR analysis was performed for the interpretation of the material's functional groups. The measurements were performed over 4000–400 cm^{-1} by obtaining each CNCs sample from both methods are mixed with dried potassium bromide (KBr) powder before subjecting to grinding. Additionally, transmission electron microscopy (TEM) was used to determine the size distributions of $CNCs_1$ and $CNCs_2$ in which they were imaged using an H-7650 Hitachi, Japan TEM. The TEM images were analyzed using Nanomeasurer 1.2 by suspending each CNCs sample in ethanol and subjecting it to ultrasonication to obtain separate crystals. Moreover, $CNCs_1$ & $CNCs_2$ were analyzed by X-ray diffraction (XRD) by using a diffractometer (D/max 2200, Rigaku, Japan) equipped with Ni-filtered Cu Kα radiation (λ = 1.5406 Å) at 40 kV and 30 mA. Recording the intensities of diffraction was done between 5° and 60° (2θ angle range) at a scan rate of 5°/min. The Segal method was used to measure the crystallinity index (CrI, %) (Aguayo et al., 2018). The crystallinity index was calculated according to Eq. (4).

$$CrI = [\frac{I200 - Iam}{I200}] \times 100 \tag{4}$$

Where I_{200} is the maximum intensity of the diffraction at peak of 200 (2θ = 22.6°) and I_{am} is the diffraction intensity at 2θ = 18°.

2.6. Cost analysis

Cost analysis was done to compare the two methods that were used for CNCs extraction from DP. The analysis was carried out by breaking down the cost of the used chemicals, materials, and energy consumed as well as other extra expenses.

3. Results and discussion

3.1. Chemical components

Table 2 shows the chemical compositions of N_1-DP, B_1-DP, N_2-DP, B_2-DP, and DP. The chemical compositions of the

Table 2 Chemical composition of the obtained cellulose nanocrystals (CNCs).

Sample	% α-Cellulose	% Hemicellulose	% Lignin
DP	21.2	28.1	19.9
Alkali treated (N_1DP)*	63.1	7.95	7.02
Alkali treated (N_2DP)*	51.5	6.7	3.21
Bleached (B_1DP)	84	2.6	0.51
Bleached (B_2DP)	72.5	1.5	0.14

*N_1DP & N_2DP (treated by NaOH), B_1DP & B_2DP (after bleaching).

intermediate products of the two methods were found to be significantly different.

The results of the chemical compositions of the DP at different treatment stages of methods 1 and 2 are listed in Table 2. It is important to note that there are other chemical components such as protein, fat, and ashes found in DP. Nevertheless, these components do not affect the isolation of CNCs due to their low percentages as reported by Genedy et al. (2017). The DP has a chemical composition of 21.2, 28.1, and 19.9% for α-cellulose, hemicellulose, and lignin, respectively (Al-Ghouti et al., 2019). The non-cellulosic content like hemicellulose has the highest percentages in comparison to the cellulose content. Therefore, the objective was to chemically treat the DP to remove the non-cellulosic contents. Hence, when the DP was subjected to treatment by NaOH, the hemicellulose and lignin contents of the DP decreased from 28.1% and 19.9% to 7.95% and 6.7%, respectively for both methods (N_1_DP & N_2_DP). On the other hand, the concentration of cellulose increased for both methods (N_1_DP & N_2-DP) to 63.1% and 51.5%, respectively. Comparing these values to the original α-cellulose of the DP, which is 21.2%, the values bare significantly high. Hence, the delignification process performed by the NaOH treatment was successful. Furthermore, it can be concluded that method 1 yields better results than method 2, in terms of chemical composition after the delignification process.

After the bleaching treatment, the hemicellulose and lignin contents decreased even more to 2.6% and 1.5%, respectively for both methods (B_1_DP & B_2_DP). Abu-Thabit et al. (2020) extracted and characterized microcrystalline cellulose from *Phoenix dactylifera* L. date seeds and found that bleached date seed has 3.92% hemicellulose and 0.86% lignin. Moreover, it can be justified that the bleaching treatment is the second treatment for the DP, therefore less hemicellulose and lignin contents are yielded. Whereas it is evident that the cellulose content for both methods (B_1_DP & B_2_DP) increased significantly to 84% and 72.5%, respectively. This can be due to the amorphous phase removal which was indicated by the presence of alkali-soluble lignin components as well as the water-soluble hemicellulose, which in turn led to the presence of higher cellulose content (Tarchoun et al., 2019). It is clear that the first method that relies on the mechanical stirrer yields better results for purified cellulose.

3.2. Physicochemical properties of $CNCs_1$ and $CNCs_2$

The physicochemical properties of $CNCs_1$ and $CNCs_2$ are listed in Table 3. Measurement of the true density of cellulosic

Table 3 Physicochemical properties of isolated CNCs.

Physicochemical property	$CNCs_1$	$CNCs_2$
True density	1.7	1.9
Moisture content (%)	5.6	6.2
pH	6.5	6.2

materials is important since it provides the required physical quantity value needed for future practical uses. The density of $CNCs_1$ (1.7) and $CNCs_2$ (1.9) are considered to be very close in value to each other. Vincent et al. (2021) used postharvest waste (stalks) to extract CNCs and found that it has a density of 1.6. In addition, comparing these results to a previous study, the true density of nanocellulose was found to be almost 1.60 regardless of the cellulose's biological origin (Daicho et al., 2019). This means that most nano-scale products have true densities that are less than 2.0 irrespective of the chemical composition and other physiochemical properties the fiber possesses. According to Crouter & Briens (2014), the moisture content is considered a significant parameter when dealing with CNCs at pilot scales such as manufacturing stages. In the current results, the measured moisture content of $CNCs_1$ is 5.6% and $CNCs_2$ 6.2%. Evans et al. (2019) extracted CNCs from sugarcane baggase and found that it has a moisture content of 3%. It can be concluded that the moisture content of method 2 is slightly higher due to the extraction step performed with hexane and water, nevertheless, there are no significant differences between both methods. This might be due to the fact that extraction in method 2 using hexane and water was used to dissolve and remove impurities that alter the properties of CNCs surfaces, these impurities include hemicelluloses, lignin, and different mono and disaccharides (Banerjee et al., 2020). Therefore, the slight moisture content may be attributed to the absorption of moisture in the spaces left vacant from the removal of hemicellulose and lignin (Sofla et al., 2016). Lastly, the pH value for the $CNCs_1$ suspension (6.4) and that of $CNCs_2$ (6.2) are close to neutral, which fulfills our aim at obtaining pure cellulose nanocrystals after modifying by sulfuric acid. Similarly, Pandi et al. (2021) synthesized cellulose nanocrystals from cotton and found that the pH of the obtained CNCs suspension was between 6 and 7.

Furthermore, considering the yield of both CNCs samples as per equation (3), $CNCs_1$ has a slightly higher yield (12%) than $CNCs_2$ (10%). Nonetheless, both methodologies presented a yield ($\geq$10%) which is considered a promising technique for CNCs production on an industrial scale (Seta et al., 2020).

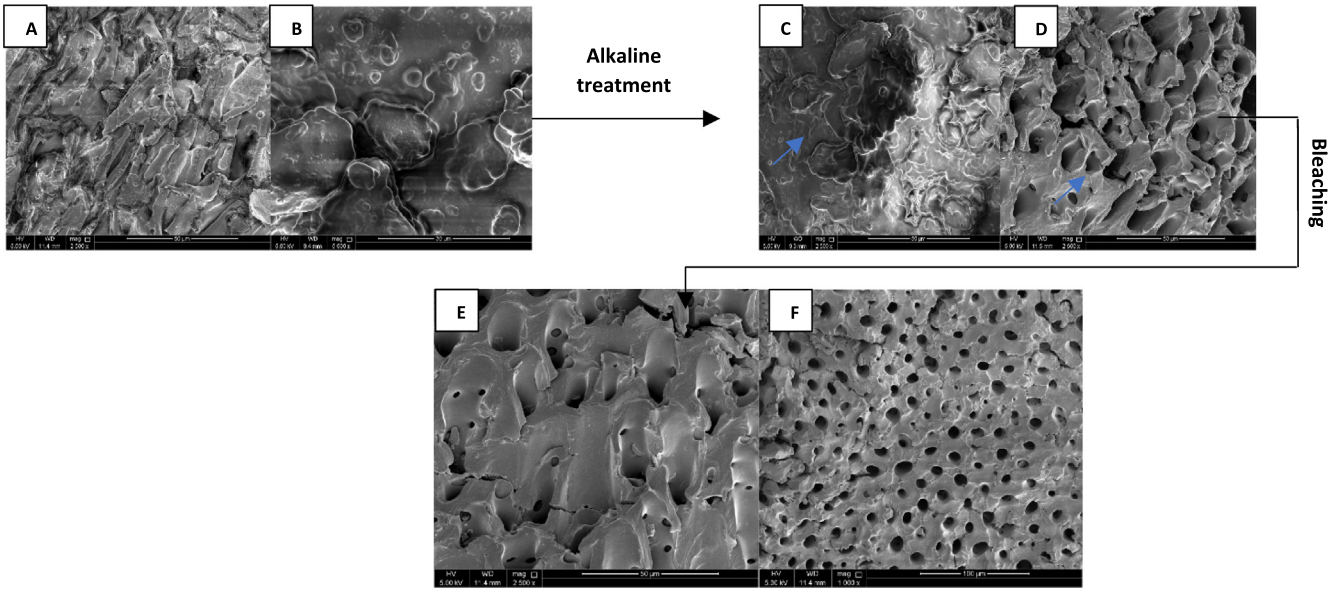

Fig. 2 Schematic illustration of SEM results of the surface morphology of A) DP at 5000x, B) DP at 2500x, C) N_1-DP, D) N_2-DP, E) B_1-DP, F) B_2-DP.

3.3. Scanning electron microscopy (SEM) analysis

The DP, N_1-DP, B_1-DP, N_2-DP, and B_2-DP were observed using a scanning electron microscope as shown in Fig. 2. The SEM images of the DP demonstrate that the sample has agglomerated and smooth surface morphology with few rough areas, which is due to the presence of hemicellulose and cellulose content that compacts and hides the cellulose fibers below them. The high magnification of the SEM image of the DP surface reveals an extremely smooth surface, which can be due to the reflection of the lignin content that coats the cell wall of the DP. Comparing this to the intermediate products of both methods (N_1-DP, N_2-DP, B_1-DP, & B_2-DP), it is evident that all the samples exhibit a rough surface with irregular morphologies because of the strong chemical treatments during the delignification and bleaching process. However, after the delignification process by NaOH, it can be inferred that the surface of both N_1-DP & N_2-DP had an irregular structure with a porous exterior. In other words, the presence of the hollow morphological surface proves the removal of the filled parts of the surface as a result of the removal of the amorphous components. Similarly, Zou et al. (2020) studied the morphology of transparent cellulose nanofibrils composites and found that the removal of cementing amorphous components led to the presence of hollow surface morphology. This can be attributed to the degradation process of the hemicellulose and the lignin content that occurred by the alkali treatment (Fu et al. 2018). Further, B_1-DP and B_2-DP exhibited porous structures, as can be shown in Fig. 2e and f. The porous morphology of the bleached samples is clear and that is due to the successful removal of hemicellulose and lignin contents. Additionally, this indicates that the removal of the residual lignin by the NaClO solution was successful. All the obtained results are also consistent with the values reported in chemical composition in Table 2. Similar results were obtained by Zheng et al. (2019), who extracted CNCs from walnut shells and found that SEM results indicate the degradation of lignin and hemicellulose due to the alkali treatment. Furthermore, Vardhini et al. (2018) investigated the effect of alkali treatment of different concentrations on the morphology of banana fiber, and SEM results indicate the removal of hemicellulose and lignin.

3.4. Transmission electron microscopy (TEM) analysis

The transmission electron microscope was used to study and observe the morphology of the cellulose nanocrystals under the two different methods. The arrangement of the cellulose nanocrystals extracted after acid hydrolysis of bleached DP is shown in Fig. 3 of both $CNCs_1$ and $CNCs_2$. The TEM was the best to study the cellulose at the nanoscale. Based on literature and previous studies, the usage of sulfuric acid at optimum concentration, temperature, and time yields ideal nanocrystals (Khan et al., 2020; Guo et al., 2020; Zheng et al., 2019). The TEM results for the $CNCs_1$ morphology after modification through sulfuric acid hydrolysis show cellulose microfibrils with packed structure because of the presence of intermolecular and intramolecular hydrogen bonding (Chen et al., 2011). It could also be due to the sonication treatment that caused the fibers to spread unevenly, but not well enough, therefore at low magnification, multiple aggregations of nanofibers are present. It is important to note that when preparing nanosize particles sufficient sonication for the sample is required to fully break the fibers into smaller microfibers (Abu-Thabit et al., 2020). Therefore, the $CNCs_1$ sample needs to be further sonicated to avoid the aggregation of the nanofibrils. Furthermore, the appearance of the aggregated nanofibrils could be due to the high specific area between the nanofibers themselves. In addition, it is evident that the fibers have rod-like morphologies, which is one of the typical cellulose nanocrystals shape (Kontturi et al., 2018). The same findings of nanocellulose TEM images obtained through sulfuric acid

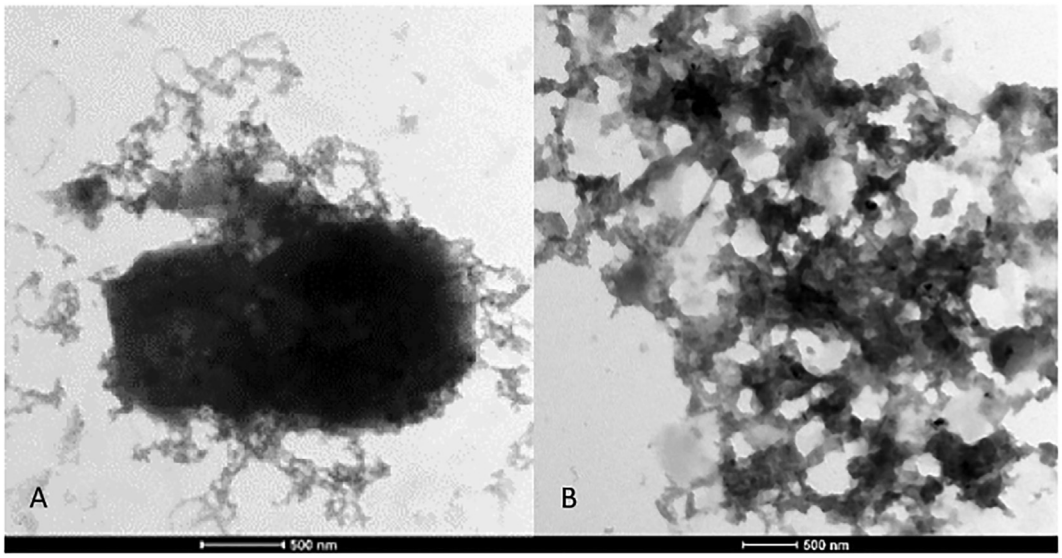

Fig. 3 TEM image of A) $CNCs_1$, B) $CNCs_2$.

hydrolysis are reported by Moreno et al., 2018. Nevertheless, at high magnification, the morphology of the nanofibers shows that the aggregates are assembled in parallel to each other and are aligned neatly alongside one another. This could be explained by the fact that the hydrogen bonds between the hydroxyl groups are found on the surface of the nanofibrils, which forces the fibers to be aligned in that way (Chen et al., 2011). Therefore, at high magnification, the appearance of the fibrils is of an organized structure. Furthermore, the ordered arrangement of the fibrils represents the crystalline region of $CNCs_1$ with few amorphous regions. This is due to the removal by sulfuric acid chemical treatment. It is worth mentioning that 64% concentration of sulfuric acid has been reported to be the best in the formation of nanocellulose and that using lower acid concentration can yield lower nanocellulose (Börjesson and Westman, 2015). As for the second methodology, it shows that the $CNCs_2$ also possesses a packed structure due to the strong hydrogen bonding. Moreover, the fibrils, in this case, are more dispersed and less clumped in comparison to $CNCs_1$, although it is similarly evident that the fibers are also rod-shaped cellulose particles. Although, as the magnification increased, the morphology of the nanofibers is shown to be assembled next to each other, where they are similar to the TEM image of $CNCs_1$. Both methods for $CNCs_1$ and $CNCs_2$ have similar morphologies, meaning that the extraction processes using both methods were applicable and successful. In the end, the size and shape of cellulose nanocrystals impact the properties it has in an aqueous media, hence these characteristics determine the application of CNCs.

3.5. Fourier transform infrared (FTIR) analysis

The importance of the FTIR spectrum relies on the fact that it demonstrates significant information regarding the chemical structure of the biopolymers obtained. The presence of multiple functionalities such as hydroxyl, methoxy, and cellulosic components were verified from the characteristic peaks detected in the FTIR spectrum of both $CNCs_1$ and $CNCs_2$ as shown in Fig. 4. This form of analysis can give us an idea of whether the extracted cellulose nanocrystals are similar in their chemical structure or whether the different methodology of extraction can reveal different chemical structures of CNCs.

Since cellulose, hemicelluloses, and lignin are the main constitutes of DP, therefore, the main functional groups present in these three materials are alkanes, esters, aromatics, ketones, and alcohols with different oxygen-containing functional groups (Chandra et al., 2016). As a result, the elimination of some peaks in the FTIR spectra will indicate the complete removal of the component's posts chemical treatment of the DP fiber. Two main absorption regions appeared in both curves, where one is at low wavelengths from 500 cm^{-1} to 1750 cm^{-1} and the other at high wavelengths from 2800 cm^{-1} to 3500 cm^{-1} (Zheng et al., 2019). Moreover, O-H stretching vibration in both samples that represent the hydrogen-bonded hydroxyl groups in the cellulose molecules is found near the region 3400 cm^{-1} as a wide broad peak. The peak intensity is reduced due to the successive treatments made by alkali and acid treatment on the DPs to obtain cellulose nanocrystals. Moreover, it can be due to the degradation of the intramolecular and intermolecular hydrogen bonds formed by most of the hydroxyl groups (Abu-Thabit et al., 2020; George & Sabapathi, 2015; Adel et al., 2011). This can also result in lower moisture absorption, hence a broad wide peak is formed (Chandra et al., 2016; Abraham et al., 2013). The peak at 1388 cm^{-1} corresponds to the bending vibrations of the C–H and C–O groups of the polysaccharides. The peak at 1155 cm^{-1} was attributed to C–O–C asymmetric stretching vibration associated with $CNCs_1$ and $CNCs_2$. Other peaks include 2851 cm^{-1} and 2920 cm^{-1} that are assigned to the C-H stretching vibrations (Abu-Thabit et al., 2020).

It is necessary to note that the FTIR results should demonstrate cellulose components since CNCs originate mainly from them. For example, the peak at 897 cm^{-1} corresponds to the C-O-C deformation and stretching in cellulose (Gonultas & Candan, 2018). In the current study, this band is found at 790 cm^{-1}, where it indicates that the original molecular struc-

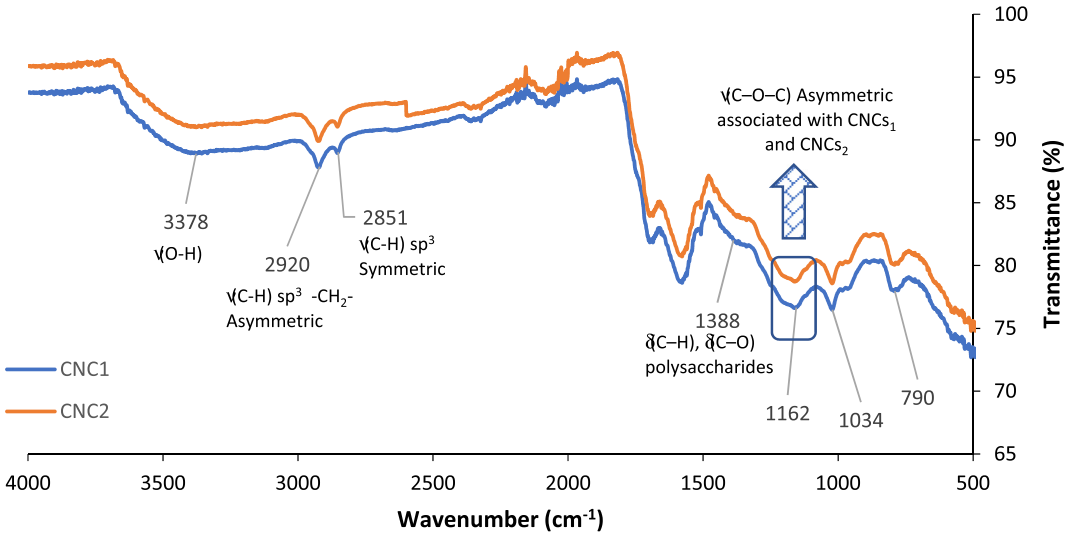

Fig. 4 FTIR spectra of $CNCs_1$ and $CNCs_2$.

ture of cellulose was still maintained even with the removal of lignin and hemicellulose components. Furthermore, the vibrations of adsorbed water molecules should be demonstrated at bands 1640 cm^{-1} (Zheng et al., 2019; Haafiz et al., 2013; Mandal & Chakrabarty, 2011). This is due to cellulose and water molecules' strong interactions with each other. However, the band is not found at that specific wavenumber. The stretching vibration of the C–O–C bonds representing the cellulose 4-glycosidic links linkages of the d-glucose units are shown at peaks 1162 cm^{-1} and 1034 cm^{-1} in both samples. These peaks correspond to the typical cellulose structure shown in previous studies (Kubovský et al., 2020; Luzi et al., 2019). It can be concluded that the modification presented by sulfuric acid that was used to obtain CNCs is successful due to the significant peaks that represent the changes in its chemical structure. The CNCs were successfully extracted from methods (1 and 2) since most of the lignin and hemicellulose components were removed. Based on the FTIR spectrum, both CNCs samples had similar chemical structures and no significant changes were observed; therefore, any isolation methods (1 and 2) can be used in the future to attain cellulose nanocrystals. The absence of peaks around 1500 cm^{-1} and 1600 cm^{-1} indicates the removal of lignin and hemicellulose (Ng et al., 2021; Mazlita et al., 2016). These results are in agreement with the results of SEM analysis that indicates the removal of lignin and hemicellulose.

3.6. X-ray powder diffraction (XRD) analysis

Biomass of lignocellulosic components is composed of amorphous and crystalline regions according to Chandra & Madakka (2019). This amorphous region is present as a result of lignin and hemicellulose present in DP, on the other hand, the crystalline region is due to the presence of cellulose. Therefore, the treatment that is done chemically leads to the depolymerization of hemicellulose and the delignification of DPs, which tends to increase the crystallinity of cellulose obtained in the end. As shown in Fig. 5, the crystallinity nature of the fibers indicates the successful conversion of the extracted cellulose to nanocellulose. The XRD spectra of $CNCs_1$ are represented by diffraction peaks at 2 theta values 15.8°, 22.5°, and 33.5°. Similarly, the diffractrogram of the $CNCs_2$ from method 2 also shows similar peaks, which are corresponding to the lattice planes (Miller index) 110, 200, and 004, respectively (Guo et al., 2020; Zheng et al., 2019; Chandra et al., 2016). It is indicated from the obtained peaks of both samples that the structure of the cellulose was preserved and maintained. Moreover, it is indicated that utilizing H_2SO_4 did not alter the original cellulose crystal (Marett et al., 2017). The high crystallinity of the obtained CNCs from both methods is indicated by the sharp diffraction peak at 22.5° which was similar to the results obtained by Trilokesh & Uppuluri (2019) who found the sharp peak at $2\theta = 22.6°$. Since hydroxyl groups formed the intermolecular and intramolecular H-bonding, therefore, the crystalline arrangement order for each CNCs has been reported. The cellulosic chains' movement is limited by the H-bonding which leads to their alignment next to each other forming the cellulose crystallinity (Chandra et al., 2016). From Eq. (4), the crystallinity index is calculated for $CNCs_1$ and $CNCs_2$ to measure if the % crystallinity changed under the two different methodologies. It was found that the apparent crystallinity of $CNCs_1$ was 69.99%, whereas the crystallinity of $CNCs_2$ was 67.79%. Furthermore, as mentioned previously, the % yield of $CNCs_1$ is slightly higher than $CNCs_2$, which could be attributed to the lower cellulose content and lower crystallinity. In general, there were no significant differences in the position of the XRD peaks between the $CNCs_1$ and $CNCs_2$. Furthermore, the consecutive chemical treatments of DP effectively removed the non-crystalline regions which caused the high crystallinity. These results support the FTIR and SEM results in terms of lignin and hemicellulose removal and confirm that the obtained product is CNCs. Table 4 represents the crystallinity percentage of our obtained CNCs and other CNCs obtained from different resources by acid hydrolysis.

3.7. Cost analysis, research implications, and limitations

Cost plays a crucial role in choosing the optimum CNCs extraction method, hence, is considered as an important driver for the success of the extraction process. Generally, assuming

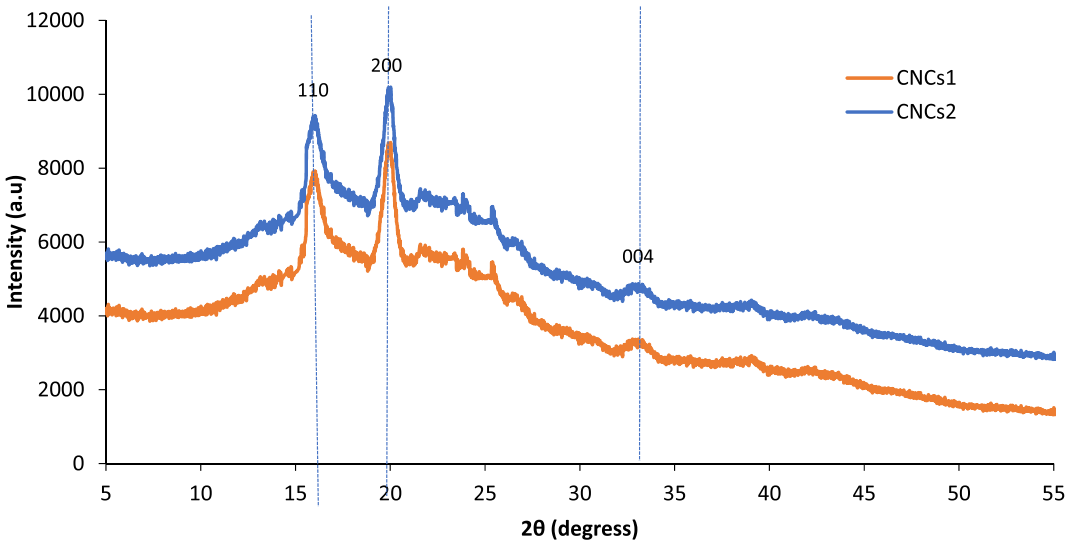

Fig. 5 XRD patterns of $CNCs_1$ and $CNCs_2$.

Table 4 Crystallinity value of cellulose nanocrystals (CNCs) obtained from different sources through acid hydrolysis.

Cellulose nanocrystal's (CNCs) source	Crystallinity (%)	Crystallinity size (nm)	References
DP ($CNCs_1$)	69.99	17.34	This Study
DP ($CNCs_2$)	67.79	17.34	This Study
Industrial bio-residue (CNCs-BR)	85.4	9.1	Herrera et al., 2012
Sugarcane peel (SP-CNCs)	99.2	25.7	Abiaziem et al., 2019
Jackfruit peel	83.42	2.80	Trilokesh & Uppuluri, 2019
Eucalyptus globulus	55.3	1.99	Carrillo et al., 2018
Eucalyptus Benthamii	54.1	1.9	Carrillo et al., 2018
Walnut shell (WS-CNCs)	40.1	–	Zheng et al., 2019
Sisal fibers	94.03	–	Sosiati et al., 2017
Sugarcane bagasse	76.89	–	Evans et al., 2019
Calotropis procera	68.7	–	Song et al., 2019

that the CNCs source is cost-effective when it does not demand high processing and it is easily available in nature, an industrial by-product, or waste material (Yaqub et al., 2014). Since the fiber business and its products reached around USD 1.08 billion in the global market, various resources have been used to produce nanocellulose. Agro-waste residues are a sustainable source of cellulosic biomass such as fruit waste, wheat straw, and date pits, in which tremendous efforts were applied for mining cellulosic fibers from such wastes (Yang et al., 2017). The cost of the extraction process can be reduced not only by using the non-valuable agricultural wastes to produce highly profitable products such as nanocellulose but also by the pretreatment process that can be performed before nanocellulose extraction. Moreover, Visanko et al., (2014) mentioned that using treatment processes such as alkaline treatment and acid hydrolysis for the production of nanocellulose instead of the highly intensive machine-driven process would reduce the required energy from 30,000 kWh/ton to 1000 kWh/ton. Based on our knowledge and the research outputs, using the Soxhlet apparatus technique (method 2) for extraction of CNCs from DP was more time consuming and energy-intensive since it required more time on the hot plate compared to the mechanical stirrer technique (method 1) as mentioned previously in the methodology. Moreover, using the Soxhlet apparatus (method 2) demanded more chemicals than the mechanical stirrer (method 1) since hexane was used only for the Soxhlet technique which increases the final cost of the extraction process. Therefore, using the mechanical stirrer technique is more cost-effective compared to the Soxhlet apparatus method.

Furthermore, sulfuric acid is commonly used for the acid hydrolysis process due to its low cost and better stability of the CNCs suspensions. However, discharging large amounts of the acid and a long time for washing the obtained CNCs is one drawback of using such acid. Considering the environmental issues caused by discharging wastewater with strong acids like sulfuric and hydrochloric acid encourages finding alternatives with less environmental impact. For this reason, phosphoric acid has been used as a promising alternative for sulfuric acid in acid hydrolysis as it showed good thermal stability, but more research is required to increase its yield, which will eventually affect the final cost of the process (Gao et al., 2020; Tang et al., 2015). The presence of hemicellulose, lignin, and other undesired organic materials present a challenge in the production of CNCs, but this can be overcome by pretreatments such as bleaching and alkaline washing which are able

Table 5 Total cost required for CNCs production under methods 1 and 2.

Item	Unit Cost (USD)	Amount used	Cost (USD)
Method 1 (Mechanical stirrer)			
Sodium hydroxide (1 kg)	40.49	30 g	1.21
Sodium hypochlorite (2.5 L)	29.4	128.57 mL	1.51
Sulfuric acid (500 mL)	26.92	168.4 mL	9.06
Dialysis bags (25 bags – Sigma-Aldrich)	134.41	1 bag	5.38
Total cost of grinding and ultrasonication	0.036 per kWh	0.064 kWh, (Energy to Heat = 0.129)	0.0023
Total cost of heating for cellulose preparation	0.036 per kWh	2.17 kWh (70℃, 6 h), (Energy to Heat at 70℃ = 0.36 kWh/hr)	0.078
Total cost of heating for CNCs preparation	0.036 per kWh	0.129 kWh (25℃, 1 h), (Energy to Heat at 25℃ = 0.129 kWh/hr)	0.004
Cost of drying	0.036 per kWh	5.88 kWh (70℃, 24 h), (Energy to Heat at 70℃ = 0.245 kWh/hr)	0.211
Net cost			17.46
Other overhead costs (10% of the net cost)			1.746
Total cost			**19.20**
Method 2 (Soxhlet apparatus)			
Hexane (1 L)	27.19	500 mL	13.6
Sodium hydroxide (1 kg)	40.49	10 g	0.40
Sodium hypochlorite (2.5L)	29.94	36.43 mL	0.42
Sulfuric acid (500 mL)	26.92	168.4 mL	9.06
Dialysis bags (25 bags – Sigma-Aldrich)	134.41	1 bag	5.38
Total cost of grinding and ultrasonication	0.036 per kWh	0.064 kWh, (Energy to Heat = 0.129 kWh/hr)	0.0023
Total cost of heating for CNCs preparation	0.036 per kWh	0.129 kWh (25℃, 1 h), (Energy to Heat at 25℃ = 0.129 kWh/hr)	0.004
Cost of drying	0.036 per kWh	5.88 kWh (70℃, 24), (Energy to Heat at 70℃ = 0.245 kWh/hr)	0.211
Net cost			29.08
Other overhead costs (10% of the net cost)			2.908
Total cost			**31.98**

to remove all these materials from the biomass. Since challenges do exist, more efficient research outputs and environmentally friendly processes are required to overcome these issues and to extract CNCs in a sustainable way.

Cost analysis for both methods was proposed by including important chemicals and materials used, energy consumption, and other expense as shown in Table 5. The cost breakdown calculations were based on 50 g of DP and the percent yields of $CNCs_1$ and $CNCs_2$ were 12% (i.e. 6 g) and 10% (i.e. 5 g). The yield is calculated and mentioned in the manuscript in Eq. (3). It was concluded that method 1 is less expensive than method 2 based on the breakdown of the cost of each step for CNCs production. Keep in mind that each extraction and isolation step of CNCs from both methods could have a potential concern regarding its sustainability towards the environment. However, future perspectives and integrated processes towards a cleaner and more sustainable approach can be achieved. For example, the dewaxing step in method 2 can be used to produce biodiesel and the black lignin solution can be used for the generation of energy (Abu-Thabit et al. 2020). Therefore, by-products produced throughout the entire production stage can be used for other purposes if the concept of sustainability is taken into consideration. This can provide a way to properly utilize residue and waste into value-added products.

4. Conclusion

The novelty of this work relies on the extraction, characterization, and comparison of CNCs from local date pits waste found in Qatar by two different extraction methods, namely mechanical stirrer and Soxhlet apparatus. Furthermore, acid hydrolysis by sulfuric acid succeeded in extracting CNCs from DP. Moreover, method 1 yields better results for purified cellulose with 84% compared to 75.2% obtained by method 2. Since the obtained CNCs by both methods had similar properties and SEM/FTIR characteristics, determining the optimum technique could be due to the cost-effectiveness, energy intake, and time consumption. Based on that it can be concluded that the mechanical stirrer technique is more cost-effective and less time-consuming compared to the Soxhlet apparatus. In the end, expanding the knowledge in the field of nanocellulose will help future product developments.

Declaration of Competing Interest

The authors declare that they have no known competing financial interests or personal relationships that could have appeared to influence the work reported in this paper.

Acknowledgment

This publication was made possible by NPRP grant # [12S-0307-190250] from the Qatar National Research Fund (a member of Qatar Foundation). The findings achieved herein are solely the responsibility of the author[s].

References

Abiaziem, C., Bassey Williams, A., Ibijoke Inegbenebor, A., Theresa Onwordi, C., Osereme Ehi-Eromosele, C., Felicia Petrik, L., 2019.

Preparation and Characterisation of Cellulose Nanocrystal from Sugarcane Peels by XRD, SEM and CP/MAS 13C NMR. Journal Of Physics: Conference Series 1299,. https://doi.org/10.1088/1742-6596/1299/1/012123 012123.

Abraham, E., Deepa, B., Pothen, L.A., Cintil, J., Thomas, S., John, M.J., Narine, S.S., 2013. Environmental friendly method for the extraction of coir fibre and isolation of nanofibre. Carbohydrate polymers 92 (2), 1477–1483.

Abu-Thabit, N. Y., Judeh, A. A., Hakeem, A. S., Ul-Hamid, A., Umar, Y., & Ahmad, A. 2020. Isolation and characterization of microcrystalline cellulose from date seeds (Phoenix dactylifera L.). *International Journal of Biological Macromolecules*, 155 (2020) 730–739.

Adel, A.M., Abd El-Wahab, Z.H., Ibrahim, A.A., Al-Shemy, M.T., 2011. Characterization of microcrystalline cellulose prepared from lignocellulosic materials. Part II: Physicochemical properties. Carbohydrate Polymers 83 (2), 676–687.

Aguayo, M., Fernández Pérez, A., Reyes, G., Oviedo, C., Gacitúa, W., Gonzalez, R., Uyarte, O., 2018. Isolation and Characterization of Cellulose Nanocrystals from Rejected Fibers Originated in the Kraft Pulping Process. Polymers 10 (10), 1145.

Alavi, M., 2019. Modifications of microcrystalline cellulose (MCC), nanofibrillated cellulose (NFC), and nanocrystalline cellulose (NCC) for antimicrobial and wound healing applications. e-Polymers 19 (1), 103–119.

Al-Ghouti, M. A., Da'ana, D., Abu-Dieyeh, M., & Khraisheh, M. 2019. Adsorptive removal of mercury from water by adsorbents derived from date pits. *Scientific reports*, *9*(1), 1-15.

Araki, J., Miyayama, M., 2020. Wet spinning of cellulose nanowhiskers; fiber yarns obtained only from colloidal cellulose crystals. Polymer 188, 122116.

Ardanuy Raso, M., Claramunt Blanes, J., Arévalo Peces, R., Parés Sabatés, F., Aracri, E., Vidal Lluciá, T., 2012. Nanofibrillated cellulose (NFC) as a potential reinforcement for high performance cement mortar composites. BioResources 7 (3), 3883–3894.

Banerjee, M., Saraswatula, S., Williams, A., Brettmann, B., 2020. Effect of purification methods on commercially available cellulose nanocrystal properties and TEMPO Oxidation. Processes 8 (6), 698.

Börjesson, M., Westman, G., 2015. Crystalline nanocellulose—preparation, modification, and properties. Cellulose-fundamental aspects and current trends, 159–191.

Brinchi, L., Cotana, F., Fortunati, E., Kenny, J.M., 2013. Production of nanocrystalline cellulose from lignocellulosic biomass: technology and applications. Carbohydrate polymers 94 (1), 154–169.

Brito, B.S., Pereira, F.V., Putaux, J.L., Jean, B., 2012. Preparation, morphology and structure of cellulose nanocrystals from bamboo fibers. Cellulose 19 (5), 1527–1536.

Camino-Sánchez, F.J., Rodríguez-Gómez, R., Zafra-Gómez, A., Santos-Fandila, A., Vílchez, J.L., 2014. Stir bar sorptive extraction: Recent applications, limitations and future trends. Talanta 130, 388–399.

Carpenter, A.W., de Lannoy, C.F., Wiesner, M.R., 2015. Cellulose nanomaterials in water treatment technologies. Environmental science & technology 49 (9), 5277–5287.

Carrillo, I., Mendonça, R.T., Ago, M., Rojas, O.J., 2018. Comparative study of cellulosic components isolated from different Eucalyptus species. Cellulose 25, 1011–1029.

Cervin, N.T., Aulin, C., Larsson, P.T., Wågberg, L., 2012. Ultra porous nanocellulose aerogels as separation medium for mixtures of oil/water liquids. Cellulose 19 (2), 401–410.

Chandra, J., George, N., Narayanankutty, S.K., 2016. Isolation and characterization of cellulose nanofibrils from arecanut husk fibre. Carbohydrate polymers 142, 158–166.

Chandra, M.R.G.S., Madakka, M., 2019. Comparative Biochemistry and Kinetics of Microbial Lignocellulolytic Enzymes. In: Recent Developments in Applied Microbiology and Biochemistry. Academic Press, pp. 147–159.

Chen, W., Yu, H., Liu, Y., 2011. Preparation of millimeter-long cellulose I nanofibers with diameters of 30–80 nm from bamboo fibers. Carbohydrate polymers 86 (2), 453–461.

Cheng, M., Qin, Z., Chen, Y., Liu, J., Ren, Z., 2017. Facile one-step extraction and oxidative carboxylation of cellulose nanocrystals through hydrothermal reaction by using mixed inorganic acids. Cellulose 24 (8), 3243–3254.

Crouter, A., Briens, L., 2014. The effect of moisture on the flowability of pharmaceutical excipients. Aaps Pharmscitech 15 (1), 65–74.

Daicho, K., Kobayashi, K., Fujisawa, S., Saito, T., 2019. Crystallinity-Independent yet Modification-Dependent True Density of Nanocellulose. Biomacromolecules 21 (2), 939–945.

Deepa, B., Abraham, E., Cordeiro, N., Mozetic, M., Mathew, A.P., Oksman, K., Pothan, L.A., 2015. Utilization of various lignocellulosic biomass for the production of nanocellulose: a comparative study. Cellulose 22 (2), 1075–1090.

Dharmalingam, K., Padmavathi, G., Kunnumakkara, A.B., Anandalakshmi, R., 2019. Microwave-assisted synthesis of cellulose/zinc-sulfate–calcium-phosphate (ZSCAP) nanocomposites for biomedical applications. Materials Science and Engineering: C 100, 535–543.

Díez, D., Urueña, A., Piñero, R., Barrio, A., Tamminen, T., 2020. Determination of Hemicellulose, Cellulose, and Lignin Content in Different Types of Biomasses by Thermogravimetric Analysis and Pseudocomponent Kinetic Model (TGA-PKM Method). Processes 8 (9), 1048.

Ditzel, F.I., Prestes, E., Carvalho, B.M., Demiate, I.M., Pinheiro, L. A., 2017. Nanocrystalline cellulose extracted from pine wood and corncob. Carbohydr. Polym. 157, 1577–1585.

Dong, S., Bortner, M.J., Roman, M., 2016. Analysis of the sulfuric acid hydrolysis of wood pulp for cellulose nanocrystal production: a central composite design study. Ind. Crop. Prod. 93, 76–87.

Dufresne, A., 2017. Nanocellulose: from nature to high performance tailored materials. Walter de Gruyter GmbH & Co KG.

Etale, A., Nhlane, D., Mosai, A. K., & Nuapia, Y. 2020. Cellulose-supported ferrihydrites for the removal of As (III), As (V) and Cr (VI) from mining-contaminated water.

Evans, S., Wesley, O., Nathan, O., Moloto, M., 2019. Chemically purified cellulose and its nanocrystals from sugarcane baggase: isolation and characterization. Heliyon 5, (10). https://doi.org/10.1016/j.heliyon.2019.e02635 e02635.

Fathi, H., El-Shazly, A., Elkady, M., Madih, K., 2018. Assessment of New Technique for Production Cellulose Nanocrystals from Agricultural Waste. Materials Science Forum 928, 83–88. https://doi.org/10.4028/www.scientific.net/msf.928.83.

Ferreira, F.V., Pinheiro, I.F., Gouveia, R.F., Thim, G.P., Lona, L.M. F., 2018. Functionalized cellulose nanocrystals as reinforcement in biodegradable polymer nanocomposites. Polymer Composites 39, E9–E29.

Fu, Q., Yan, M., Jungstedt, E., Yang, X., Li, Y., Berglund, L., 2018. Transparent plywood as a load-bearing and luminescent biocomposites. *Composites Science and Technol*ogy 164, 296–303.

Gao, A., Chen, H., Tang, J., Xie, K., Hou, A., 2020. Efficient extraction of cellulose nanocrystals from waste Calotropis gigantea fiber by SO42-/TiO2 nano-solid superacid catalyst combined with ball milling exfoliation. Industrial Crops And Products 152, 112524.

García, A., Gandini, A., Labidi, J., Belgacem, N., Bras, J., 2016. Industrial and crop wastes: A new source for nanocellulose biorefinery. Industrial Crops and Products 93, 26–38.

George, J., Sabapathi, S.N., 2015. Cellulose nanocrystals: synthesis, functional properties, and applications. Nanotechnology, science and applications 8, 45.

Gonultas, O., Candan, Z., 2018. Chemical characterization and ftir spectroscopy of thermally compressed eucalyptus wood panels. Maderas. Ciencia y tecnología 20 (3), 431–442.

Guo, Y., Zhang, Y., Zheng, D., Li, M., Yue, J., 2020. Isolation and characterization of nanocellulose crystals via acid hydrolysis from

agricultural waste-tea stalk. International Journal of Biological Macromolecules 163, 927–933.
Haafiz, M.M., Eichhorn, S.J., Hassan, A., Jawaid, M., 2013. Isolation and characterization of microcrystalline cellulose from oil palm biomass residue. Carbohydrate polymers 93 (2), 628–634.
Herrera, M.A., Mathew, A.P., Oksman, K., 2012. Comparison of cellulose nanowhiskers extracted from industrial bio-residue and commercial microcrystalline cellulose. Materials Letters 71, 28–31.
Hosseini, M., Dizaji, H.Z., Taghavi, M., Babaei, A.A., 2020. Preparation of ultra-lightweight and surface-tailored cellulose nanofibril composite cryogels derived from Date palm waste as powerful and low-cost heavy metals adsorbent to treat aqueous medium. Industrial crops and products 154, 112696.
Isik, M., Sardon, H., Mecerreyes, D., 2014. Ionic liquids and cellulose: dissolution, chemical modification and preparation of new cellulosic materials. International journal of molecular sciences 15 (7), 11922–11940.
Isogai, A., Saito, T., Fukuzumi, H., 2011. TEMPO-oxidized cellulose nanofibers. nanoscale 3 (1), 71–85.
Jafari, H., Shahrousvand, M., Kaffashi, B., 2020. Preparation and characterization of reinforced poly (ε-caprolactone) nanocomposites by cellulose nanowhiskers. Polymer Composites 41 (2), 624–632.
Jawaid, M., Mohammad, F. (Eds.), 2017. Nanocellulose and Nanohydrogel Matrices: Biotechnological and Biomedical Applications. John Wiley & Sons.
Jung, S.J., Kim, S.H., Chung, I.M., 2015. Comparison of lignin, cellulose, and hemicellulose contents for biofuels utilization among 4 types of lignocellulosic crops. Biomass and bioenergy 83, 322–327.
Kambli, N., Mageshwaran, V., Patil, P., Saxena, S., Deshmukh, R., 2017. Synthesis and characterization of microcrystalline cellulose powder from corn husk fibres using bio-chemical route. Cellulose 24 (12), 5355–5369. https://doi.org/10.1007/s10570-017-1522-4.
Khalil, H.A., Tye, Y.Y., Leh, C.P., Saurabh, C.K., Ariffin, F., Fizree, H.M., Suriani, A.B., 2018. Cellulose reinforced biodegradable polymer composite film for packaging applications. In: Bionanocomposites for packaging applications. Springer, Cham, pp. 49–69.
Khan, M.N., Rehman, N., Sharif, A., Ahmed, E., Farooqi, Z.H., Din, M.I., 2020. Environmentally benign extraction of cellulose from dunchi fiber for nanocellulose fabrication. International Journal of Biological. Macromolecules.
Khattab, T.A., Fouda, M.M., Rehan, M., Okla, M.K., Alamri, S.A., Alaraidh, I.A., Allam, A.A., 2020. Novel halochromic cellulose nanowhiskers from rice straw: Visual detection of urea. Carbohydrate Polymers 231, 115740.
Kian, L.K., Saba, N., Jawaid, M., Sultan, M.T.H., 2019. A review on processing techniques of bast fibers nanocellulose and its polylactic acid (PLA) nanocomposites. International journal of biological macromolecules 121, 1314–1328.
Kontturi, E., Laaksonen, P., Linder, M.B., Gröschel, A.H., Rojas, O. J., Ikkala, O., 2018. Advanced materials through assembly of nanocelluloses. Advanced Materials 30 (24), 1703779.
Kubovský, I., Kačíková, D., Kačík, F., 2020. Structural Changes of Oak Wood Main Components Caused by Thermal Modification. Polymers 12 (2), 485. https://doi.org/10.3390/polym12020485.
Lani, N., Ngadi, N., Johari, A., Jusoh, M., 2014. Isolation, Characterization, and Application of Nanocellulose from Oil Palm Empty Fruit Bunch Fiber as Nanocomposites. J. Nanomater., 1–9
Li, J., Wei, X., Wang, Q., Chen, J., Chang, G., Kong, L., Liu, Y., 2012. Homogeneous isolation of nanocellulose from sugarcane bagasse by high pressure homogenization. Carbohydrate polymers 90 (4), 1609–1613.
Li, R., Fei, J., Cai, Y., Li, Y., Feng, J., Yao, J., 2009. Cellulose whiskers extracted from mulberry: A novel biomass production. Carbohydrate Polymers 76 (1), 94–99. https://doi.org/10.1016/j.carbpol.2008.09.034.
Li, Y., Xiao, H., Pan, Y., Wang, L., 2018. Novel composite adsorbent consisting of dissolved cellulose fiber/microfibrillated cellulose for dye removal from aqueous solution. ACS Sustainable Chemistry & Engineering 6 (5), 6994–7002.
Luque-Garcıa, J.L., De Castro, M.L., 2004. Focused microwave assisted Soxhlet extraction: devices and applications. Talanta 64 (3), 571–577.
Lusiana, S. E., Aisiyah, M. M., Nasihin, Z. D., Srihardyastutie, A., Rahman, M. F., & Masruri, M. 2019, November. Biocellulose isolated from the waste of pinecone flower (Pinus merkusii Jungh Et De Vriese). In *Journal of Physics: Conference Series* (Vol. 1374, No. 1, p. 012022). IOP Publishing.
Luzi, F., Puglia, D., Sarasini, F., Tirillò, J., Maffei, G., Zuorro, A., et al, 2019. Valorization and extraction of cellulose nanocrystals from North African grass: Ampelodesmos mauritanicus (Diss). Carbohydrate Polymers 209, 328–337. https://doi.org/10.1016/j.carbpol.2019.01.048.
Lyne, B. 2013. Market prospects for nanocellulose. *The Royal Institute of Technology, Alberta Biomaterials Development Centre, Edmunton, AB, Canada.*
M.A. Genedy, A., Othman Shalaby, A., & F. El-Mehiry, H. (2017). Date pits: Chemical composition and sensory characteristics for developins value added product. *Research Journal Specific Education*, *2017*(45), 673-592. https://doi.org/10.21608/mbse.2017.139077
Magalhães, W., Cao, X., Lucia, L., 2009. Cellulose Nanocrystals/Cellulose Core-in-Shell Nanocomposite Assemblies. Langmuir 25 (22), 13250–13257. https://doi.org/10.1021/la901928j.
Mandal, A., Chakrabarty, D., 2011. Isolation of nanocellulose from waste sugarcane bagasse (SCB) and its characterization. Carbohydrate Polymers 86 (3), 1291–1299. https://doi.org/10.1016/j.carbpol.2011.06.030.
Marett, J., Aning, A., Foster, E.J., 2017. The isolation of cellulose nanocrystals from pistachio shells via acid hydrolysis. Ind. Crop. Prod. 109, 869–874.
Mazlita, Y., Lee, H., Hamid, S., 2016. Preparation of Cellulose Nanocrystals Bio-Polymer from Agro-Industrial Wastes: Separation and Characterization. Polymers And Polymer Composites 24 (9), 719–728. https://doi.org/10.1177/096739111602400907.
Medina, L., Nishiyama, Y., Daicho, K., Saito, T., Yan, M., Berglund, L.A., 2019. Nanostructure and Properties of Nacre-Inspired Clay/Cellulose Nanocomposites—Synchrotron X-ray Scattering Analysis. Macromolecules 52 (8), 3131–3140.
Meyabadi, T.F., Dadashian, F., Mohamad, S., Asl, E., 2014. Spherical cellulose nanoparticles preparation from waste cotton using a green method. Powder Technology 261, 232–240.
Moreno, G., Ramirez, K., Esquivel, M., Jimenez, G., 2018. Isolation and Characterization of Nanocellulose Obtained from Industrial Crop Waste Resources by Using Mild Acid Hydrolysis. Journal of Renewable Materials 6 (4), 362–369.
Nabili, A., Fattoum, A., Passas, R., Elaloui, E., 2016. Extraction and characterization of cellulose from date seeds (Phoenix dactylifera L.). Cellulose. Chem. Technol. 50, 10151023.
Ng, L., Wong, T., Ng, C., Amelia, C., 2021. A review on cellulose nanocrystals production and characterization methods from Elaeis guineensis empty fruit bunches. Arabian Journal Of Chemistry 14, (9). https://doi.org/10.1016/j.arabjc.2021.103339 103339.
Ogungbenro, A.E., Quang, D.V., Al-Ali, K.A., Vega, L.F., Abu-Zahra, M.R.M., 2018. Physical synthesis and characterization of activated carbon from date seeds for CO2 capture. Journal of Environmental Chemical Engineering 6, 4245–4252.
Pandi, N., Sonawane, S., Anand Kishore, K., 2021. Synthesis of cellulose nanocrystals (CNCs) from cotton using ultrasound-assisted acid hydrolysis. Ultrasonics Sonochemistry 70,. https://doi.org/10.1016/j.ultsonch.2020.105353 105353.
Peretz, R., Sterenzon, E., Gerchman, Y., Vadivel, V.K., Luxbacher, T., Mamane, H., 2019. Nanocellulose production from recycled paper mill sludge using ozonation pretreatment followed by

recyclable maleic acid hydrolysis. Carbohydrate polymers 216, 343–351.
Phanthong, P., Reubroycharoen, P., Hao, X., Xu, G., Abudula, A., Guan, G., 2018. Nanocellulose: Extraction and application. Carbon Resources Conversion 1 (1), 32–43.
Rajinipriya, M., Nagalakshmaiah, M., Robert, M., Elkoun, S., 2018. Importance of agricultural and industrial waste in the field of nanocellulose and recent industrial developments of wood based nanocellulose: a review. ACS Sustainable Chemistry & Engineering 6 (3), 2807–2828.
Ribeiro, R.S.A., Bojorge, N., Pereira Jr, N., 2020. Statistical analysis of the crystallinity index of nanocellulose produced from Kraft pulp via controlled enzymatic hydrolysis. Biotechnology and Applied. Biochemistry.
Ribeiro, R.S., Pohlmann, B.C., Calado, V., Bojorge, N., Pereira Jr, N., 2019. Production of nanocellulose by enzymatic hydrolysis: Trends and challenges. Engineering in Life Sciences 19 (4), 279–291.
Sacui, I.A., Nieuwendaal, R.C., Burnett, D.J., Stranick, S.J., Jorfi, M., Weder, C., Gilman, J.W., 2014. Comparison of the properties of cellulose nanocrystals and cellulose nanofibrils isolated from bacteria, tunicate, and wood processed using acid, enzymatic, mechanical, and oxidative methods. ACS applied materials & interfaces 6 (9), 6127–6138.
Seta, F.T., An, X., Liu, L., Zhang, H., Yang, J., Zhang, W., Liu, H., 2020. Preparation and characterization of high yield cellulose nanocrystals (CNC) derived from ball mill pretreatment and maleic acid hydrolysis. Carbohydrate polymers 234, 115942.
Shafizah, S., Izwan, A. S., Fatirah, F., & Hasraf, M. N. 2018, October. Review on cellulose nanocrystals (CNCs) as reinforced agent on electrospun nanofibers: mechanical and thermal properties. In *IOP Conference Series: Materials Science and Engineering*. *IOP Publishing* (p. 012011).
Shanmugarajah, B., Kiew, P.L., Chew, I.M.L., Choong, T.S.Y., Tan, K.W., 2015. Isolation of nanocrystalline cellulose (NCC) from palm oil empty fruit bunch (EFB): Preliminary result on FTIR and DLS analysis. Chemical Engineering Transactions 45, 1705–1710.
Silva, L. E., dos Santos, A. D. A., Torres, L., McCaffrey, Z., Klamczynski, A., Glenn, G., ... & Damásio, R. A. P. 2020. Redispersion and structural change evaluation of dried microfibrillated cellulose. *Carbohydrate Polymers*, 117165.
Sofla, M.R.K., Brown, R.J., Tsuzuki, T., Rainey, T.J., 2016. A comparison of cellulose nanocrystals and cellulose nanofibres extracted from bagasse using acid and ball milling methods. Advances in Natural Sciences: Nanoscience and Nanotechnology 7, (3) 035004.
Song, K., Zhu, X., Zhu, W., Li, X., 2019. Preparation and characterization of cellulose nanocrystal extracted from Calotropis procera biomass. Bioresources And Bioprocessing 6 (1).
Song, Q., Winter, W.T., Bujanovic, B.M., Amidon, T.E., 2014. Nanofibrillated cellulose (NFC): A high-value co-product that improves the economics of cellulosic ethanol production. Energies 7 (2), 607–618.
Sosiati, H., Wijayanti, D., Triyana, K., & Kamiel, B. 2017. Morphology and crystallinity of sisal nanocellulose after sonication. 10.1063/1.4999859
Syafri, E., Kasim, A., Abral, H., Sulungbudi, G.T., Sanjay, M.R., Sari, N.H., 2018. Synthesis and characterization of cellulose nanofibers (CNF) ramie reinforced cassava starch hybrid composites. International journal of biological macromolecules 120, 578–586.
Tang, L., Huang, B., Lu, Q., Wang, S., Qu, W., Lin, W., Chen, X., 2013. Ultrasonication-assisted manufacture of cellulose nanocrystals esterified with acetic acid. Bioresource technology 127, 100–105.
Tang, Y., Shen, X., Zhang, J., Guo, D., Kong, F., Zhang, N., 2015. Extraction of cellulose nano-crystals from old corrugated container fiber using phosphoric acid and enzymatic hydrolysis followed by sonication. Carbohydrate Polymers 125, 360–366.
Tarchoun, A., Trache, D., Klapötke, T., 2019. Microcrystalline cellulose from Posidonia oceanica brown algae: Extraction and characterization. International Journal Of Biological Macromolecules 138, 837–845. https://doi.org/10.1016/j.ijbiomac.2019.07.176.
Trache, D., Hussin, M.H., Chuin, C.T.H., Sabar, S., Fazita, M.N., Taiwo, O.F., Haafiz, M.M., 2016. Microcrystalline cellulose: Isolation, characterization and bio-composites application—A review. International Journal of Biological Macromolecules 93, 789–804.
Trilokesh, C., Uppuluri, K.B., 2019. Isolation and characterization of cellulose nanocrystals from jackfruit peel. Scientific Reports 9, 16709. https://doi.org/10.1038/s41598-019-53412-x.
Visanko, M., Liimatainen, H., Sirviö, J.A., Heiskanen, J.P., Niinimäki, J., Hormi, O., 2014. Amphiphilic cellulose nanocrystals from acid-free oxidative treatment: physicochemical characteristics and use as an oil–water stabilizer. Biomacromolecules 15, 2769–2775.
Wahib, S. A., Da'na, D. A., Ashfaq, M. Y., AL-Ghouti, M. A. 2021. Functionalized cellulose nanocrystals as a novel adsorption material for removal of boron from water. *Case studies in chemical and environmental engineering, 4,* 100121.
Wahib, S. A., Da'na, D. A., Zaouri, N., Hijji, Y. M., AL-Ghouti, M. A. 2022. Adsorption and recovery of lithium ions from groundwater using date pits impregnated with cellulose nanocrystals and ionic liquid. *Journal of hazardous materials*, *421*, 126657.
Wang, J., Liu, X., Jin, T., He, H., Liu, L., 2019. Preparation of nanocellulose and its potential in reinforced composites: a review. Journal of Biomaterials Science, Polymer Edition 30 (11), 919–946.
Wulandari, W., Rochliadi, A., Arcana, I., 2016. Nanocellulose prepared by acid hydrolysis of isolated cellulose from sugarcane bagasse. IOP Conference Series: Materials Science and Engineering 107, 012045.
Yagub, M., Sen, T., Afroze, S., Ang, H., 2014. Dye and its removal from aqueous solution by adsorption: A review. Advances In Colloid And Interface Science 209, 172–184.
Yang, X., Wang, X., Liu, H., Zhao, Y., Jiang, S., Liu, L., 2017. Impact of dimethyl sulfoxide treatment on morphology and characteristics of nanofibrillated cellulose isolated from corn husks. *Bioresource Technol*ogy 12, 95–106.
Zheng, D., Zhang, Y., Guo, Y., Yue, J., 2019. Isolation and characterization of nanocellulose with a novel shape from walnut (Juglans Regia L.) shell agricultural waste. Polymers 11 (7), 1130.
Zou, W., Wang, Z., Sun, D., Ji, X., Zhang, P., Zhu, Z., 2020. Transparent Cellulose Nanofibrils Composites with Two-layer Delignified Rotary-cutting Poplar Veneers (0°-layer and 90°-layer) for Light Acquisition of Solar Cell. Scientific Reports 10 (1). https://doi.org/10.1038/s41598-020-58941-4.